FLOW INSTABILITIES IN A GRAFT ANASTOMOSIS: FLOW REYNOLDS NUMBER 350

Colin J. Bates & Andrew Grand
Cardiff School of Engineering
Cardiff University, PO Box 685
Cardiff CF24 3TA, UK
BatesCJ@Cardiff.ac.uk

Joanna L Bates
Department of Radiology
Hull Royal Infirmary, Anlaby Road, Hull
East Yorkshire, HU3 2JZ, UK
JoBates@Doctors.net.uk

ABSTRACT

The major cause of arterial bypass graft failure is intimal hyperplasia. Low and fluctuating wall shear stresses in the graft, which are associated with disturbed flow, are believed to be an important factor in the development and localisation of intimal hyperplasia.

This study presents details of the flow structure inside a 30° Y-junction, various fillet radii at the intersection between the graft and the host artery have been investigated. Reynolds numbers, based upon water as the working fluid, and pulsatile frequencies (shown in brackets) of 125(0.7 Hz), 230(0.85 Hz) and 350(1 Hz) have been studied together with various **D**istal **O**utlet **S**egment to **P**roximal **O**utlet **S**egment (**DOS**:**POS**) flow ratios. The measurements confirm the presence of all the anticipated flow features normally associated with low Reynolds number pulsatile flow through a bifurcation, such as: -

(a) the flow impacting the floor of the host artery, as it flows through the junction.
(b) the position where the inlet flow impacted the junction floor was governed by the DOS:POS flow ratio, the fillet radius and the mean Reynolds number.
(c) fluctuating wall shear stresses in the toe, heel and the base of the host artery of the graft.
(d) the existence and longevity of single, double and triple vortices at various phases of each individual pulsatile cycle.

INTRODUCTION

Abnormal haemodynamic factors have been strongly linked to the onset of diseases, such as atherosclerosis, hyperplasia and thrombosis. This abnormal flow behaviour can occur in bends and bifurcations of medium to large arteries. Details of specific sites, in end-to-side distal anastomoses, where intimal hyperplasia has been observed at the heel and toe of the graft together with the floor of the host artery has been presented by Sottiurai et al (1989). Their drawings, particularly in the toe region, show the extent of intimal hyperplasisa to be effectively around the whole circumference. They conclude that intimal hyperplasia was not a scar tissue, but created and remodelled by the influence of blood flow dynamics. Flow visualisation pictures clearly demonstrate qualitatively the variations in the flow velocities and the three dimensional nature of the pulsatile flow within end to side vascular graft anastomoses (Bassiouny et al 1992, White et al 1993, Fisher et al 2001). The papers by Bassiouny et al (1992) and White et al (1993) report studies undertaken on similar geometries, with the graft parallel to the host artery, no indication being given with respect to the local radius between them. Hood length to host artery diameter ratios of approximately 4:1 (Bassiouny et al 1992, White et al 1993) and 8:1 (Fisher et al 2001) were investigated under both steady and pulsatile flow conditions. Flow visualisation pictures, based upon a sheet of light generated by a low powered helium neon laser and photographic images, show the important flow features which vary appreciable throughout the pulsatile cycle. These pictures clearly show the presence of a stagnation point, on the floor of the graft and its movement axially throughout the pulsatile cycle. A vortex was also identified in the vicinity of the heel junction, between the host artery and the graft, it was also observed to move within the hood over each pulsatile cycle, breaking up during early diastole (Bassiouny et al 1992). Interestingly, White et al (1993) reported the presence of a transient separation region along the anatomotic hood, near to the toe, this flow separation was observed with both the 4:1 and 8:1 hood length to host artery diameter ratios. For the larger 8:1 ratio this hood wall flow separation was evident with the100:0 DOS:POS flow ratio, although for the 4:1 ratio wall separation was reported for the 0:100 and 50:50 DOS:POS ratios, but not the 100:0 and 80:20 ratios. Fisher et al (2001) provide evidence of the flow structure in pre cuffed grafts, using flow visualisation and Doppler ultrasound techniques. A pre cuffed graft Reynolds number of 146 was employed together with DOS:POS ratios of 100:0 and 50:50. The complexity of the flow field over a biphasic flow cycle was reported together with the existence of the associated vortical flow structure.

The visualisation pictures presented by Bassiouny et al 1992, White et al 1993 and Fisher et al 2001 show these

important flow features in the illuminated central plane through both the host artery and the graft, no flow features were presented for the perpendicular plane through the host artery at the junction with the graft.

Non intrusive photochromic dye techniques and laser illumination were employed by Ojha et al (1990) to provide details of the flow field in the host artery, with the proximal portion upstream of the 45° graft completely occluded (DOS:POS ratio 100:0). Both steady and pulsatile flows were investigated over a Reynolds number range from 250 to 1300. As a result of their detailed investigation they provided a sketch of the three dimensional double helix observed to be present in the flow immediately downstream of the anastomoses site. Particle Image Velocimetry (PIV) results presented by Bates et al (2001) showed the three dimensional time dependent pulsatile flow features within a similar configuration at Reynolds numbers of 500 and above, the angle between the graft and host artery was 30°, however three specific radii were investigated, at the heel of the graft, namely 5 mm, 15 mm and 25 mm.

The current paper seeks to provide clear quantitative evidence of the importance of the flow dynamics, particularly in the horizontal plane through the host artery. The existence of single, double and triple vortices have been observed and their longevity throughout the pulsatile cycle determined. Three inlet graft Reynolds numbers (125, 230 and 350) have been studied, together with five radii (0, 5, 10, 20 and 25 mm) between the heel of the 30° graft and the host artery. The heel fillet radius is a variable which has not been studied previously over this Reynolds number range. The detailed results currently presented cover a DOS:POS ratio of 50:50, the 10 mm fillet radius and the 350 Reynolds number, the results show the size and strength of the vortices, as well as their stimulation and decay over the 1 Hz pulsatile cycle.

EXPERIMENTAL TECHNIQUES

Five idealised scaled models of an arterial bypass anastomosis were manufactured from 50 mm internal diameter QVF transparent glass. These were used to study the flow structure within a 30° Y-junction with a heel fillet radius of 0, 5, 10, 20 or 25 mm.

Full details of the constant head flow facility have been presented previously in the literature (Bates et al 1999). A fully developed sinusoidal wave pulsatile flow was supplied by a Watson-Marlow high flow peristaltic pump. Three Reynolds numbers and pulse frequencies of 125 (0.7 Hz), 230 (0.85 Hz) and 350 (1 Hz) were investigated. At these Reynolds numbers and pulse frequencies two flow ratios, between the distal outlet segment (DOS) and the proximal outlet segment (POS), were studied 100:0 and 50:50. Reynolds number was defined as:-

$$\mathrm{Re} = \frac{\bar{u}\, d}{\nu} \quad ,$$

$\bar{u}$ being the bulk mean velocity, d the internal pipe diameter and ν the kinematic viscosity.

The flow characteristics through the junction were then monitored non-intrusively using PIV techniques, which allowed the measurement of the instantaneous two-dimensional velocity field.

For this study, a Dantec FlowMap PIV system was used, details of which have been published previously (Bates et al 2001).

The PIV images were collected at a framing rate of 15 Hz, this represents a time interval of 66.7 ms between successive frames. Based upon this framing rate and the 1 Hz frequency of the pulsatile flow 15 PIV pictures were captured each cycle during the 350 Reynolds number measurements. This pulsatile frequency and pipe configuration provides a high value for the Womersley parameter of 62.7.

The perspex viewing box employed previously to totally encase the 30° Y-junction (Bates et al 2001) was not used, due to the introduction of a carefully designed geometric template, comprising a regular array of black dots of known spacing, and a new software algorithm. This template was laminated, to prevent water damage, and mounted in the horizontal plane within the pipeline, which was subsequently filled with water. A frame of the template was then recorded employing the same optical configuration and camera setting, which would be used for the PIV measurements in this plane. This procedure was repeated for the vertical plane. The distortion due to the curvature was established via the use of this template and two *dewarping* algorithms determined. These *dewarping* software algorithms were subsequently employed in order to reduce the light distortion caused by the pipe's curvature. Unfortunately due to the curvature of the QVF glass, in the wall region, some distortion was still experienced.

RESULTS - Velocity vectors

PIV measurements in both the vertical and horizontal planes were undertaken to investigate the flow structure inside the 30° Y-junction over the pulsatile cycle. The PIV measurements obtained were instantaneous near real time whole velocity fields. The PIV velocity fields viewed by the optical arrangement were not large enough to span the whole length of the junction, therefore four different frame regions were investigated. The four regions were positioned around a central datum plane, which was taken to be the intersection of the centreline of the bypass graft with that of the host artery, as shown in Figure 1. Figure 1 also shows the designation of the individual regions, one frame on the distal side of this central plane (region 1), with three regions (designated 2, 3 and 4) on the proximal side. As Figure 1 shows each region was 80 mm long and 50 mm wide. Region 1 includes a 6.7 mm length of the hood on the distal side of the datum, prior to the toe, where the inlet jet enters or reverse flow occurs into the hood. On the proximal side of the datum Figure 1 shows that regions 2 and 3 cover the remainder of the inlet jet up to and including the influence of the fillet radius, shown as 10 mm in Figure 1. The fillet radius employed controlled the value of the anastomotic hood length to host diameter ratio, for these experiments the ratio ranged from 2 up to 3.86, being 2.72 for the 10 mm fillet radius depicted in Figure 1. Fifty individual successive PIV frames were taken. Detailed results based on the experimental measurements will focus on the highest Reynolds number (350) and the 10 mm fillet radius.

(a) Instantaneous velocity fields - DOS:POS ratio 50:50

(i) Vertical Plane

The instantaneous velocity vectors for the vertical plane of region 2 are shown in Figure 2, Figure 2 (a) shows the inlet flow at peak systole, the maximum velocity vector being 0.0211 m/s at a position –71.6 mm proximal from the datum and 27.45 mm up from the base, the angle of the inlet jet being 58.6°. As shown by boxed region D no recirculation into the hood is evident, although a clear cross flow exists (box C), due to the strength of the inlet jet, which extends distally into region 1 on the lower left hand side. Half a cycle later at minimum diastole, as shown in Figure 2 (b), the cross flow (boxed region C1) has changed to be such that the flow, on the left hand side, enters this plane from region 1 across the datum, with strong distal flow across the datum into region 1 adjacent to the bottom wall. The recirculation flow into the hood now consists of strong vectors, (boxed region D1) with a peak vector velocity of 0.0021 m/s, the surrounding region, in this plane is shown to be a quiescent envelope of fluid. This incoming flow could be caused by the initial inlet jet impacting upon the floor further upstream, as a result of the local curvature the flow would divide and spiral around the wall.

Instantaneous distal axial velocity profiles for region 2, -45.2 mm proximally from the datum, half a cycle apart are shown in Figure 3. A smooth profile is evident at minimum diastole with a peak velocity of 0.0075 m/s, together with the presence of a small negative flow into the hood. As expected the higher velocities are shown at peak systole with smooth wall profiles, no flow into the hood and a flat unsheared peak velocity region of 0.011 m/s.

(ii) Horizontal Plane

The corresponding instantaneous velocity vectors for region 2, in the horizontal plane at peak systole, are shown in Figure 4 (a). No vortices are evident at this instant, although their locations are clearly identified in the flow field. At the right hand side of the figure the inflow is shown to be from the two side walls, boxed regions E and E1, coupled with a strong inflow from region 3 over the central core region (box E2) on the right hand side. This central core strengthens to give a peak velocity of 0.012 m/s, at a location of –53.3 mm proximally from the datum and 26.6 mm up from the lower wall. On the left hand side of the figure the flow exits axially near the walls across the datum into region 1, with a significant cross flow in the distal sense over the remainder of the region in between this axial wall flow.

Interestingly in the horizontal plane at minimum diastole Figure 4 (b) shows two vortices to be now well established, although not quite symmetrically positioned with respect to the centreline. A strong inlet flow across the datum from region 1 is evident (box F2), this proximal flow interacts with the central inlet jet (box F3) which emanates from region 3. These two opposing flows interact with a stagnation point being shown in this plane around which the flow divides forming the two vortices. Strong flow, denoted by boxes F and F1, driven by the strong inlet flow across the datum from region 1, is entrained into the inlet jet from region 3 (box F3). The peak absolute velocity between the two vortices has decayed to 0.006443 m/s at a location of –55.6 mm proximally and 22.75 mm up from the lower side wall.

The instantaneous distal axial velocity profiles at a position –44.6 mm proximally from the datum are shown in Figure 5, this position represents the plane through the *eye* of the upper vortex prior to its decay, as shown in Figure 4 (b). Figure 5 shows a lack of symmetry at both peak systole and minimum diastole, both profiles display the same overall features with the greater velocities as expected at peak systole. Across this plane the presence of a strong central distal core flow over a complete cycle is evident, at minimum diastole the peak value falls to 0.0051 m/s compared with 0.011 m/s at peak systole. The wall regions for both profiles show only positive distal flow at peak systole, whereas negative velocities exist at minimum diastole these negative velocities in the wall regions both extend to almost one third of the diameter.

The vertical plane of region 3, as shown in Figure 1, covers the 10 mm fillet radius as well as the heel region of the anastomosis. Figure 6 displays typical instantaneous velocity vectors in the horizontal plane of region 3. Resolution of any absolute velocity vectors, which are normal to the walls in the vertical plane, causes the velocity to be zero in the horizontal plane; this is confirmed in Figure 6. On the centreline the vectors are shown to flow distally and proximally away from this zero velocity or stagnation point. The strong jet inflow into this horizontal plane from region 2 (boxes G1 and G2) are present over the whole cycle, they bifurcate around the zero velocity point to become aligned so as to flow either distally as an inlet jet into region 2 (box G3) or proximally into region 4, with remarkable symmetry being displayed by the proximal flow about the axial centreline. The peak axial velocity vectors, which flow into region 2 from within box G3, vary over the 1 Hz pulsatile cycle being 0.00536 m/s at systole and 0.00233 m/s at diastole.

DISCUSSION

The instantaneous PIV velocity profiles provide flow details, which have not previously been reported in the literature, these measurements show the instantaneous velocity variations, which occur over a complete pulsatile cycle. In the vertical plane recirculation into the hood region, prior to the toe, was shown to occur over the diastole half of the cycle for both the 100:0 and 50:50 DOS:POS flow ratios. This confirms the observations of White et al (1993), although the current hood length to host artery diameter ratio was only 2.72:1 compared with 4:1. This phenomenon was *washed out* during the systole half of the cycle. Similarly for the 50:50 DOS:POS flow ratio the heel vortex flow was shown to enter the fillet area during the diastole phase of the cycle, with a wall stagnation point present downstream of the intersection of the fillet radius with the host artery. This stagnation point was observed to move over a distance of -132.8 to -140.5 mm proximally from the datum (the intersection of the fillet radius and the host artery occurs at a position -130.6 mm proximally from the datum). Due to this flow feature during the systole phase of the cycle the shear stress, on this upper wall, will be in the proximal sense up to the stagnation point and in the distal sense thereafter. Estimates of the instantaneous shear stress in the wall region, in the horizontal plane of region 2 at the four corners (identified as A, B, C and D in Figure 1), were determined from the near wall velocity gradient. The numerical values of the shear stress, even with some wall distortion, correlate well with those that

would be experienced near the wall of a 50 mm diameter pipe with a fully developed laminar flow at the corresponding Reynolds number. The profiles at B and C showed that for the -80 mm position the shear stresses were in the same sense over the whole cycle. However at A and D the direction of the shear stress changed, for 30% and 20% of the cycle respectively, from the proximal to the distal sense. Ojha et al (1990) and White et al (1993) have reported similar shear stress variations in the wall region of their arterial anastomosis models. At the four corners of region 2 (denoted A, B, C and D in Figure 1) the estimated shear stresses varied in magnitude from +0.0003 N/m^2 to –0.00002 N/m^2 over a pulsatile cycle. Inspection of the individual PIV instantaneous velocity fields, over a complete cycle, enabled the presence, extent and longevity of individual vortices, as well as the size of the toe and heel recirculation regions to be established. In the horizontal plane of region 2, for the 50:50 DOS:POS flow ratio, no vortices were observed for two successive frames, a single vortex was observed either side of the these two successive zero vortex frames, this part of the cycle represents the late acceleration, peak systole and early deceleration. Three vortices were present during the late deceleration and early acceleration phases of the pulsatile cycle 72° before and after minimum diastole, over the remaining acceleration, deceleration and diastole phases of the cycle two vortices were recorded. Small variations in the peak velocity was recorded between the acceleration and deceleration phases either side of minimum diastole, over the systole half of the cycle no peak velocity variations were evident. Back flow from region 1 across the datum into region 2 was only observed over the diastole half of the cycle, thereby providing the stimulus to drive the vortices.

CONCLUSIONS

The results, for the 10 mm fillet radius between the heel junction of the graft and host artery, confirm the existence over each pulsatile cycle, at a Reynolds number of 350, of single, double and triple vortices in the horizontal plane below the hood. Triple vortices were recorded at the middle of both the acceleration and deceleration phases of the cycle. At peak systole no vortices were recorded, the velocity of the inlet jet displayed peak velocity vectors and recirculation into the hood at both the toe and heel intersections did not occur. During all the other phases of the pulsatile cycle recirculation into the hood was experienced, with fluid being drawn from region 1 past the toe of the graft into the hood as well as from around the fillet radius of the heel. This hood entrainment and its variation over the pulsatile cycle cause rapid changes in the magnitude and direction of the shear stress in both the vertical and horizontal planes at these toe and heel locations.

REFERENCES

Bassiouny, H. S., White, S., Glagov, S., Choi, E., Giddens, D. P. and Zarins, C. K., 1992, "Anastomotic intimal hyperplasia: Mechanical injury or flow induced", *Journal of Vascular Surgery*, Vol. 15, pp. 708-717.

Bates, C. J., O'Doherty, D. M. and Williams, D., 1999, "Experimental and computational modelling of flow through an arterial bypass graft". In *Cardiovascular Flow Modelling and Measurement with Application to Clinical Medicine* (Eds S. G. Sajjadiu, G. B. Nash and M. W. Rampling), Oxford University Press.

Bates, C. J., O'Doherty, D. M. and Williams, D., 2001, "Flow instabilities in a graft anastomosis: a study of the instantaneous velocity fields", *Proc Instn Mech Engrs*, Vol. 215 Part H, pp. 579-587.

Fisher, R. K., How, T. V., Toonder, I. M., Hoedt, M. T. C., Brennan, J. A., Gilling-Smith, G. L. and Harris P. L., 2001, "Harnessing haemodynamic forces for the suppression of anastomotic intimal hyperplasia: the rationale for precuffed grafts", *Eur J Vasc Endovasc Surg*, Vol. 21, pp. 520-528.

Ojha M., Ethier C. R., Johnston K. W. and Cobbold, S. C., 1990, "Steady and pulsatile flow fields in an end-to-side arterial anastomosis model", *Journal of Vascular Surgery*, Vol. 12, pp. 747-753.

Sottiurai, V. S., Yao, J. S. T., Batson, R. C., Sue, S. L., Jones, R. and Nakamura, Y. A., 1989, "Distal anastomotic intimal hyperplasia: histopathologic character and biogenesis", *Ann. of Vascular Surgery*, Vol. 3(1), pp. 26-33.

White, S. S., Zarins, C. K., Giddens, D. P., Bassiouny, H. S., Loth, F., Jones, S. A. and Glagov, S., 1993, "Haemodynamic patterns in two flow models of end to side vascular graft anastomoses: Effect of pulsatility, flow division, Reynolds number and hood length", *Journal of Biomechanial Engineering*, Vol. 115, pp. 104-111.

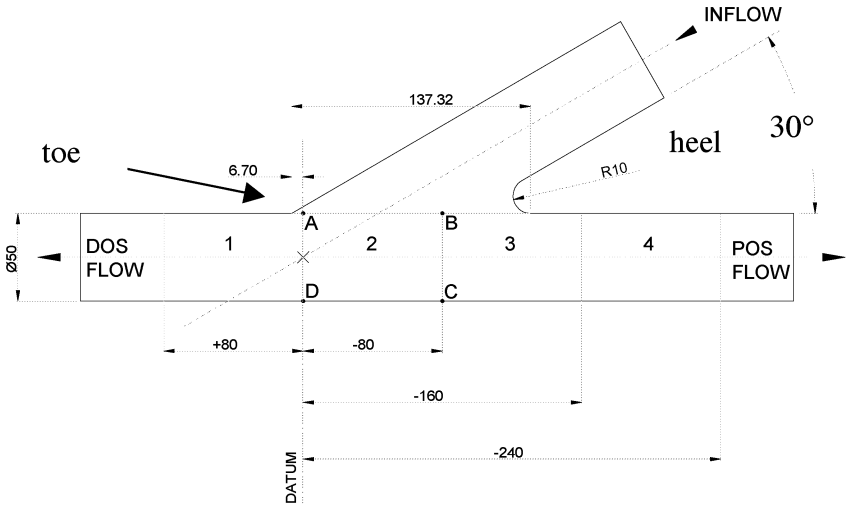

All dimensions in mm

Figure 1 Line diagram showing the vertical cross-section of the 30° junction of the anastomosis with the horizontal host artery , regions 1, 2, 3 and 4 have been identified together with the datum

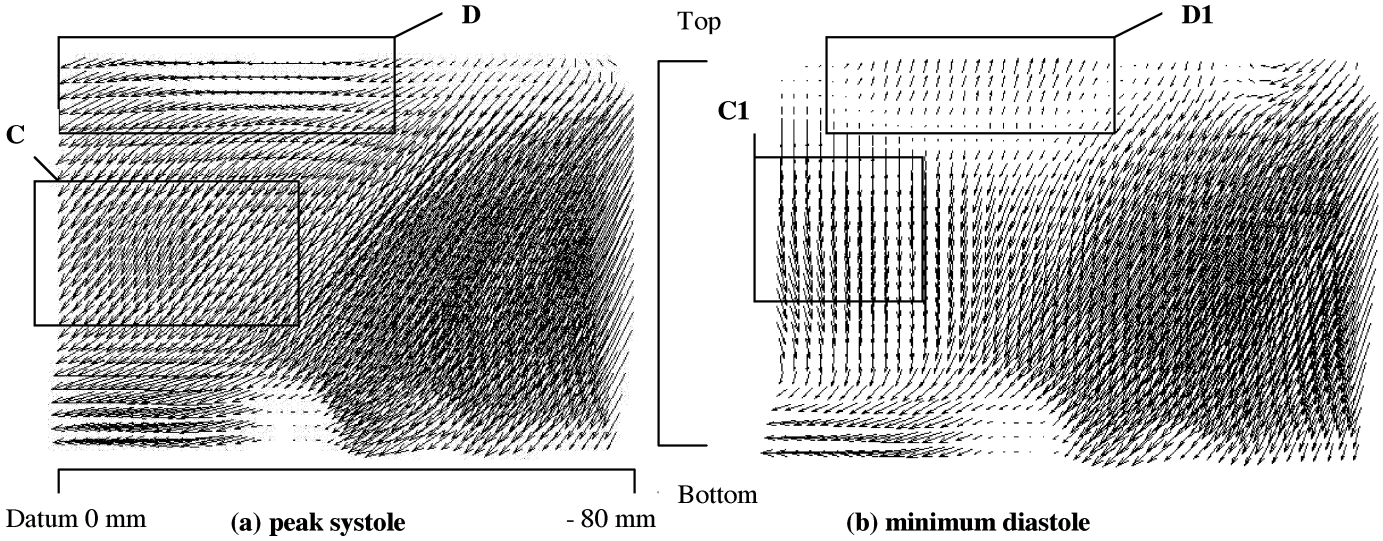

Figure 2 DOS:POS ratio 50:50, instantaneous velocity vectors in the inlet jet in the vertical plane of region 2

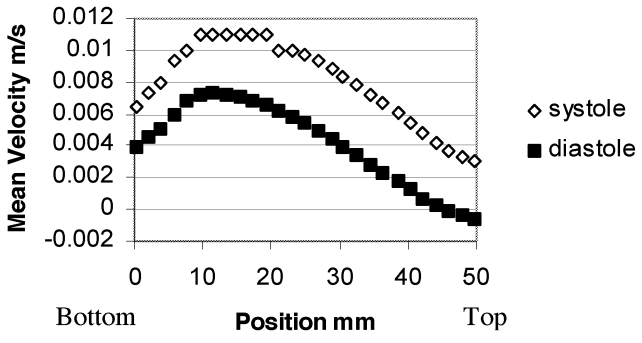

Figure3 DOS:POS ratio 50:50, instantaneous distal axial velocity profiles in the vertical plane of region 2 at a point – 45.2 mm proximally from the datum

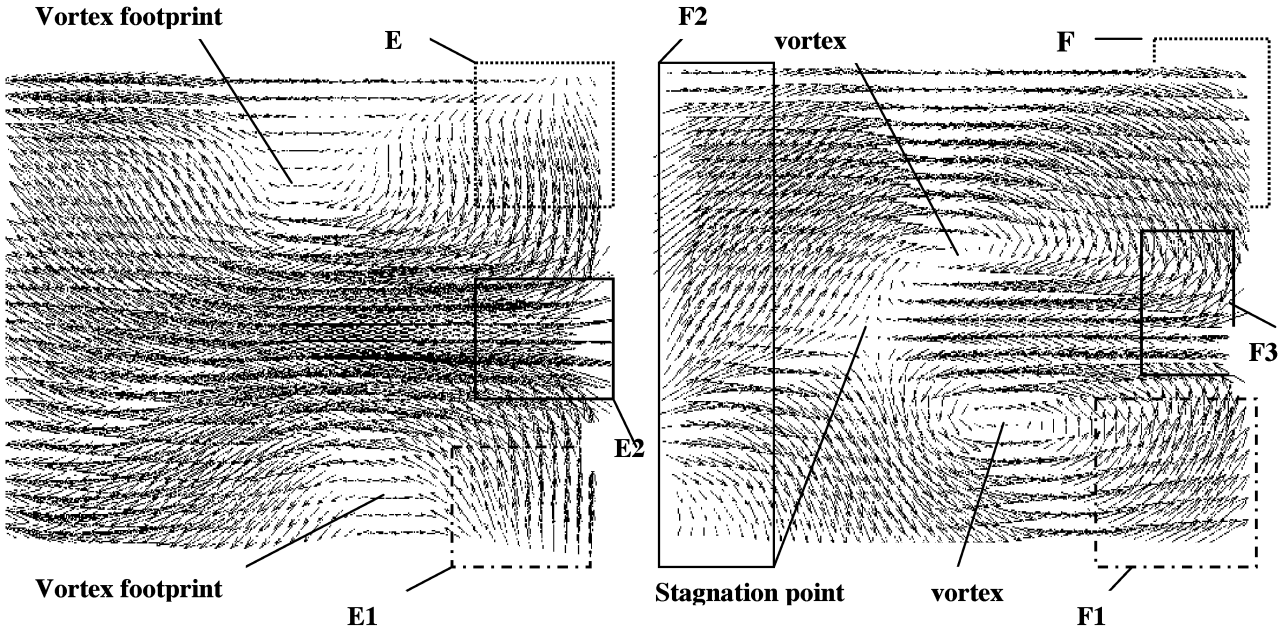

Figure 4 DOS:POS ratio 50:50, instantaneous velocity vectors in the inlet jet in the horizontal plane of region 2

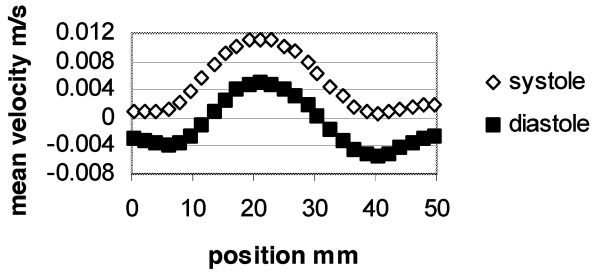

Figure 5 DOS:POS ratio 50:50, instantaneous distal axial velocity profiles in the horizontal plane of region 2 at a point – 44.6 mm proximally from the datum

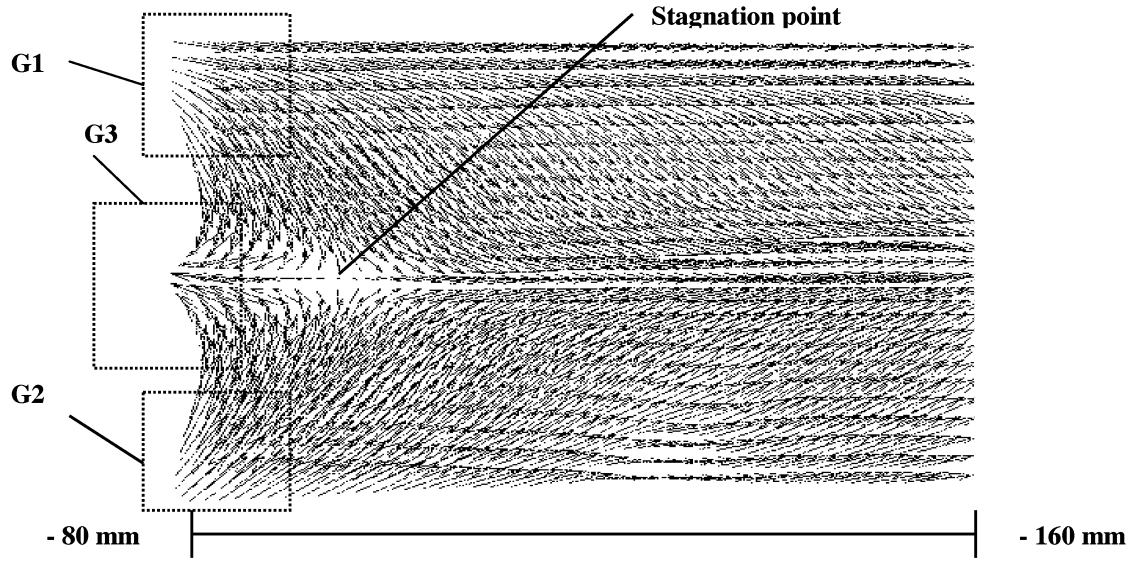

Figure 6 DOS:POS ratio 50:50 instantaneous velocity vectors in the horizontal plane of region 3